(article starts on next page)

Redesign and reconstruction of a mevalonate pathway and its application in terpene production in *Escherichia coli*

Bo Hyun Choi[a], Jin Ho Kim[a], Sun Young Choi[a], Se Jong Han[b], Pyung Cheon Lee[a],*

[a] *Department of Molecular Science and Technology, Ajou University, Woncheon-dong, Yeongtong-gu, Suwon 16499, South Korea*
[b] *Division of Polar Life Sciences, Korea Polar Research Institute, Incheon, South Korea*

ABSTRACT

Metabolic engineering of heterologous biosynthetic pathways in microbial hosts is an alternative way for producing high-value biochemicals. Here, heterologous mevalonate (MVA) and prenyl pyrophosphate (IPP) pathways of a new isolate *Enterococcus kingsejongensis* Gf1 were redesigned and reconstructed in *Escherichia coli*. Two MVA upstream enzymes of *E. kingsejongensis* Gf1 were functionally expressed and overexpression of the two enzymes led to a yield of 52.5 g/L MVA after 65 h of fed-batch fermentation. Next, the functions of three MVA downstream enzymes were verified by addition of exogenous MVA. Finally, whole MVA pathway enzymes and IPP pathway enzymes were combined in *E. coli* in order to overproduce squalene and β-carotene. The *E. coli* strains coexpressing entire MVA and IPP pathway enzymes enhanced squalene production by 15-fold and β-carotene production by 2.5-fold.

1. Introduction

A large number of natural products can be utilized as value-added industrial materials, such as therapeutic drugs, cosmetics and food ingredients, and biochemicals/biofuels. The rapid growth of the biochemical industry has alleviated general limitations by technical development, securing of novel organic sources, and utilization of renewable feedstock, such as raw glycerol waste (Chaudhary et al., 2012; Sadhukhan et al., 2016). Isoprenoids are a representative subclass of diverse natural compounds; however, most of the isoprenoids are produced in low quantities by plants and are difficult to obtain with high purity from extracts. Moreover, chemical synthesis of isoprenoids is difficult and expensive because of the structural complexity of isoprenoids (Gliszczyńska et al., 2017; Hung et al., 2018). Alternatively, diverse isoprenoids pathways have been metabolically engineered in heterologous microbial hosts to produce various valuable isoprenoid compounds (Ward et al., 2018; Wang et al., 2017). Engineered microbial hosts have been successfully utilized to produce valuable isoprenoids at an industrial scale, and hence, such hosts are potentially beneficial to the environment and can change the trends of isoprenoid production.

However, limited supply of precursors for heterologous isoprenoids biosynthesis in microbial hosts is one of the major limiting factors in the large-scale production of isoprenoids.

Structurally, isoprenoid molecules are comprised of unique five carbon backbone structures, which derive from two precursors: C_5 isopentenyl pyrophosphate (IPP) and C_5 dimethylallyl pyrophosphate (DMAPP). The C_5 precursor molecules are synthesized by either the MEP pathway (2-*C*-methyl-D-erythritol 4-phosphate pathway) or the mevalonate (MVA) pathway in nature (Tholl, 2015). Seven enzymes are involved in the MEP pathway to synthesize IPP and DMAPP from two glycolytic intermediates, pyruvate and glyceraldehyde-3-phosphate (G3P), whereas six enzymes of the MVA pathway synthesize IPP and DMAPP from acetyl-CoA (Hunter, 2007; Miziorko, 2011) (Fig. 1). IPP and DMAPP are mainly utilized for synthesis of prenyl pyrophosphates, which are used for cell wall and quinone biosynthesis (Connolly and Winkler, 1989).

Engineering of the endogenous MEP pathway, such as balancing G3P and pyruvate pool and overexpressing MEP pathway enzymes, enhanced yields of isoprenoids in *E. coli* strains (Li et al., 2018; Yang et al., 2018). Similar to the MEP pathway, engineering of the heterologous MVA pathway also increased isoprenoid production in *E. coli* strains (Li et al., 2019; Liu et al., 2019).

Enterococcus strains have been known to synthesize IPP via an MVA pathway (Lee and Schmidt-Dannert, 2002) and the *Enterococcus* MVA pathway enzymes showed higher activity than enzymes from other microbial sources (Kim and Lee, 2012; Lee et al., 2008; Yang et al., 2012). Although MVA enzymes of *E. faecalis* have been frequently used
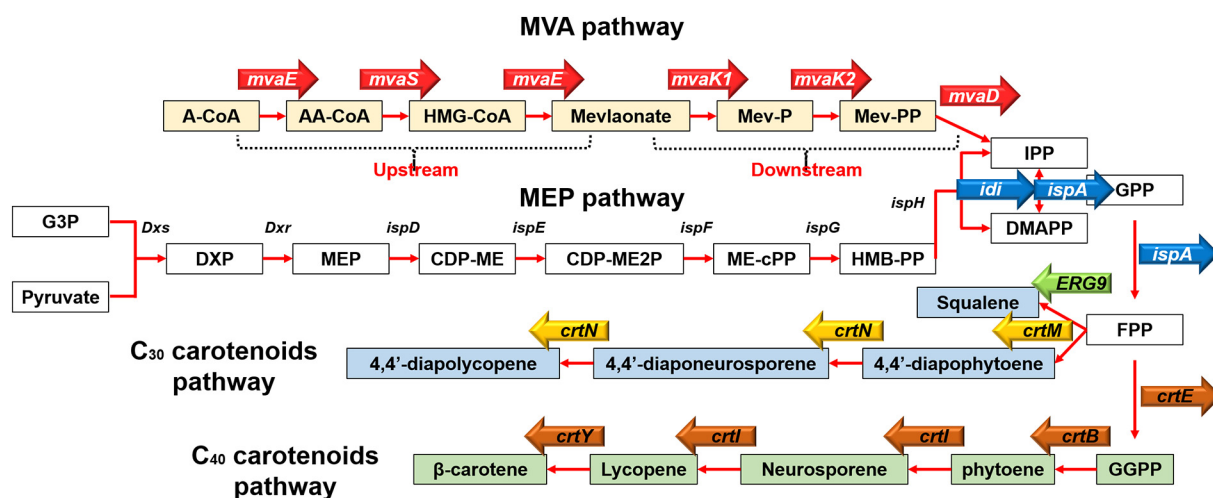
Fig. 1. Biosynthesis of carotenoids and squalene via the MEP or MVA (MVA) pathway. Synthetic expression modules used in this study are represented by an arrow with a corresponding gene name. Genes and their corresponding enzymes (all genes were obtained from *E. kingsejongensis* Gf1 unless otherwise stated) - mvaE: acetoacetyl-CoA thiolase/HMG-CoA reductase (Hedl et al., 2002) from *E. faecalis* or *E. kingsejongensis*; mvaS: HMG-CoA synthase from *E. faecalis* or *E. kingsejongensis* Gf1; mvaK1: MVA kinase, mvaK2: phosphoMVA kinase, mvaD: MVA pyrophosphate decarboxylase, and idi: IPP isomerase from *E. coli* or *E. kingsejongensis* Gf1; ispA: FPP synthase and ERG9: squalene synthase from *S. cerevisiae* AH109; crtM: 4,4′-diapophytoene synthase from *S. aureus*; crtN: 4,4′-diapophytoene desaturase from *S. aureus*; crtE: GGPP synthase from *P. agglomerans*; crtB: phytoene synthase from *P. agglomerans*; crtI: phytoene desaturase from *P. agglomerans*; and crtY: lycopene cyclase from *P. agglomerans*. Pathway intermediates: G3P, glyceraldehyde 3-phosphate; DXP, 1-deoxy-D-xylulose 5-phosphate; MEP, 2-*C*-methyl-D-erythritol 4-phosphate; CDP-ME, 4-diphosphocytidyl-2-*C*-methyl-D-erythritol; CDP-ME2P, 4-diphosphocytidyl-2-*C*-methyl-D-erythritol 2-phosphate; ME-cPP, 2-*C*-methyl-D-erythritol 2,4-cyclopyrophosphate; HMB-PP, 1-hydroxy-2-methyl-2-(*E*)-butenyl 4-pyrophosphate; IPP, isopentenyl pyrophosphate; DMAPP, dimethylallyl pyrophosphate; GPP, geranyl pyrophosphate; FPP, farnesyl pyrophosphate; GGPP, geranylgeranyl pyrophosphate; A-CoA, acetyl-CoA; AA-CoA acetoacetyl-CoA; HMG-CoA, hydroxymethylglutaryl-CoA; Mev-P, MVA 5-phosphate; and Mev-PP, MVA pyrophosphate.

in heterologous isoprenoid production, enzymes with higher activity are still required for industrial-scale production.

In this study, the activity and function of a heterologous MVA pathway and IPP pathway enzymes of *E. kingsejongensis* Gf1, recently isolated from the gut of an Antarctic South Polar Brown Skua, were investigated in *E. coli*. The MVA and IPP pathway enzymes of *E. kingsejongensis* Gf1 exhibit high activities, and thus, the recombinant *E. coli* strains coexpressing entire MVA and IPP pathway enzymes exhibited enhanced yields of squalene and β-carotene.

2. Materials & methods

2.1. Plasmid construction

Escherichia coli XL1-Blue was used for all cloning and expression analyses. Genomic DNA of *E. faecalis* KCTC3206, *E. kingsejongensis* Gf1, and *S. cerevisiae* AH109 were isolated using the gDNA extraction kit (Macrogen, Korea), and used for gene cloning to construct the mevalonate, prenyl pyrophosphate, and squalene pathways. For amplifying genes of each pathway, PCR primers were designed based on corresponding gene sequences from GenBank database. The eight genes (*mvaS*, *mvaE*, *mvaK1*, *mvaK2*, *mvaD*, *ERG9*, *idi*, and *ispA*) were obtained with the primers: mvaS-F (5′-GCTCTAGAAGGAGGATTACAAAATGAC AATTGGGATTGATAA-3′), mvaS-R (5′-CCGGAATTCTTAGTTTCGATAA GAACGAA-3′), mvaE-F (5′–GCTCTAGAAGGAGGATTACAAATTGAAAA CAGTAGTTATTAT-3′), mvaE-R (5′-TTC CCTTGCGGCCGCTTATTGTTT TCTTAAATCATTT-3′), mvaK1-F (5′– GCTCTAGAAGGAGGATTACAAA ATGAATATAAAAAAACAAGGC-3′), mvaK1-R (5′-CCGGAATTCTTACTT TTTCACCTCTAATGA-3′), mvaK2-F (5′– GCTCTAGAAGGAGGATTACA AAATGATTGAAGTTACTACG -3′), mvaK2-R (5′-CCGGAATTCTCATCT TTTCGATTCATGC-3′), mvaD-F (5′–GCTCTAGAAGGAGGATTACAAAA TGGATTCAATCATTAGAGG-3′), mvaD-R (5′-TTCCCTTGCGGCCGCTTA TTTATCCATTCCTTTCGTTTCAA-3′), ERG9-F (5′–CGGGATCCAGGAGG ATTACAAAATGGGAAAGCTATTACAATT-3′), ERG9-R (5′-GCTCTAGAT CATAAAGTGTATATATAATAAAA-3′), idi-F (5′-GCTCTAGAAGGAGGA TTACAAAATGGTCAAAAGGAGTGT-3′), idi-R (5′-GCGAATTCTTAACG

TTTTGCGAAAACT-3′), ispA-F (5′-GCTCTAGAAGGAGGATTACAAAAT GACGAATTTTAGTCAAC-3′), and ispA-R (5′-GCGCCATGGCTATCTCAA TTGTAACTGA-3′). The PCR products of 10 genes encoding HMG-CoA synthase (mvaS) and acetoacetyl-CoA thiolase/HMG-CoA reductase (mvaE) of *E. faecalis*, HMG-CoA synthase (mvaS), acetoacetyl-CoA thiolase/HMG-CoA reductase (mvaE), mevalonate kinase (mvaK1), phosphormevalonate kinase (mvaK2), mevalonate-5-diphosphate decarboxylase (mvaD), isopentenyl-diphosphate isomerase (IDI), and farnesyl diphosphate synthase (IspA) of *E. kingsejongensis* Gf1, and squalene synthase (ERG9) of *S. cerevisiae* AH109 were then cloned into the high copy plasmid pUCM (Kim et al., 2010), which was modified to facilitate the constitutive expression of the cloned gene. Then, genes, together with a modified constitutive *lac*-promoter and a ribosome binding site, were sequentially subcloned to assemble from pUCM_X (X, a pathway gene) into the low copy plasmid pBBR1MCS2 or pSTVM, which was modified from pSTV28 vector by deleting *lacZα* fragment and *lac*-promoter. As there was no sequence information available on these genes, the five MVA pathway genes were obtained using primers designed based on corresponding gene sequences from *E. faecalis* KCTC3206. After obtaining the five MVA pathway genes (mvaS$_{f1}$, mvaE$_{f1}$, mvaK1$_{f1}$, mvaK2$_{f1}$, and mvaD$_{f1}$) of *E. kingsejongensis* Gf1, each gene was modulated to be individually expressed in the pUCM vector, leading to development of pUCM-mvaS$_{f1}$, pUCM-mvaE$_{f1}$, pUCM-mvaK1$_{f1}$, pUCM-mvaK2$_{f1}$, and pUCM-mvaD$_{f1}$ (Table 1). To assemble the five MVA pathway enzymes as a modular system, the genes were divided into two groups: an 'upstream' pathway which converts acetyl-CoA to MVA in three enzymatic steps, leading to development of pSTVM-mvaE$_{f1}$-mvaS$_{f1}$, and a 'downstream' pathway which transforms MVA to IPP in three enzymatic steps, leading to development of pSTVM-mvaK1$_{f1}$-mvaK2$_{f1}$-mvaD$_{f1}$ (Fig. 1 and Table 1). Finally, five individual modules were assembled into the pSTVM vector to develop pSTVM-mvaE$_{f1}$-mvaS$_{f1}$-mvaK1$_{f1}$-mvaK2$_{f1}$-mvaD$_{f1}$ plasmid for the *E. kingsejongensis* Gf1 whole MVA pathway expression in *E. coli*. In addition, two genes encoding IPP isomerase (idi$_{f1}$) and FPP synthase (ispA$_{f1}$) of *E. kingsejongensis* Gf1 were engineered to be individually expressed in the pUCM vector, leading to development of pUCM-idi$_{f1}$ and pUCM-

Table 1

Strains and plasmids used in this study.

Strains and plasmids	Relevant properties	Source or reference
Strains		
Enterococcus faecalis	MVA pathway	KCTC 3206
Enterococcus kingsejongensis Gf1	MVA pathway	This study
Saccharomyces cerevisiae AH109	Squalene pathway	Takara
Pantoea agglomerans	C40 carotenoids pathway	KCTC 2479
Staphylococcus aureus	C30 carotenoids pathway	KCTC 3881
Escherichia coli JM109	EndA1 glnV44 thi-1 relA1 gyrA96 recA1 mcrB+ Δ(lac-proAB) e14- [F′ traD36 proAB+ lacI^q lacZΔM15] hsdR17(r$_K^-$ m$_{/k}^+$)	New England BioLabs
Escherichia coli top 10	F$^-$ mcrA Δ(mrr-hsdRMS-mcrBC) φ80lacZΔM15 ΔlacX74 nupG recA1 araD139 Δ(ara-leu)7697 galE15 galK16 rpsL(Str^R) endA1λ$^-$	Invitrogen
Escherichia coli XL1-Blue	EndA1 gyrA96(nalR) thi-1 recA1 relA1 lac glnV44 F′[::Tn10 proAB+ laclq Δ(lacZ)M15] hsdR17 (rK- mK+)	Stratagene
MVA1	XL1-Blue harboring pUCM_*mvaE*f1 and pSTVM_*mvaS*f1 from *E. kingsejongensis* Gf1	This study
MVA2	XL1-Blue harboring pUCM_*mvaS*f1 and pSTVM_*mvaE*f1 from *E. kingsejongensis* Gf1	This study
MVA3	XL1-Blue harboring pSTVM_*mvaS*f1_*mvaE*f1 from *E. kingsejongensis* Gf1	This study
MVA4	XL1-Blue harboring pUCM_*mvaS*f1_*mvaE*f1 from *E. kingsejongensis* Gf1	This study
MVA5	XL1-Blue harboring pUCM_*mvaE*Ef and pSTVM_*mvaS*Ef from *E. faecalis*	This study
MVA6	XL1-Blue harboring pSTVM_*mvaK1*f1_*mvaK2*f1_*mvaD*f1 from *E. kingsejongensis* Gf1 and pBBR-*crtM*SA-*crtN*SA from *S. aureus*	This study
MVA7	XL1-Blue harboring pSTVM_*mvaK1*f1_*mvaK2*f1_*mvaD*f1 from *E. kingsejongensis* Gf1 and pUCM_*crtE*PA_*crtB*PA_*crtI*PA_*crtY*PA_*crtZ*PA_*crtX*PA from *P. agglomerans*	This study
MVA8	XL1-Blue harboring pUCM_*ERG9*SC from *S. cerevisiae* AH109	This study
MVA9	XL1-Blue harboring pUCM_*ERG9*SC from *S. cerevisiae* AH109 and pSTVM_*mvaS*f1_*mvaE*f1_*mvaK1*f1_*mvaK2*f1_*mvaD*f1 from *E. kingsejongensis* Gf1	This study
MVA10	XL1-Blue harboring pUCM_*ERG9*SC from *S. cerevisiae* AH109, pSTVM_*mvaS*f1_*mvaE*f1_*mvaK1*f1_*mvaK2*f1_*mvaD*f1 from *E. kingsejongensis* Gf1, and pBBRM1MCS-2_*idi*JM from *E. coli* JM109	This study
MVA11	XL1-Blue harboring pUCM_*ERG9*SC from *S. cerevisiae* AH109, pSTVM_*mvaS*f1_*mvaE*f1_*mvaK1*f1_*mvaK2*f1_*mvaD*f1 from *E. kingsejongensis* Gf1, and pBBRM1MCS-2_*ispA*T10 from *E. coli* Top10	This study
MVA12	XL1-Blue harboring pUCM_*ERG9*SC from *S. cerevisiae* AH109, pSTVM_*mvaS*f1_*mvaE*f1_*mvaK1*f1_*mvaK2*f1_*mvaD*f1 from *E. kingsejongensis* Gf1, and pBBRM1MCS-2_*idi*JM_*ispA*T10 from *E. coli* JM109 and Top10	This study
MVA13	XL1-Blue harboring pUCM_*ERG9*SC from *S. cerevisiae* AH109, pSTVM_*mvaS*f1_*mvaE*f1_*mvaK1*f1_*mvaK2*f1_*mvaD*f1, and pBBRM1MCS-2_*idif*1 from *E. kingsejongensis* Gf1	This study
MVA14	XL1-Blue harboring pUCM_*ERG9*SC from *S.cerevisiae* AH109, pSTVM_*mvaS*f1_*mvaE*f1_*mvaK1*f1_*mvaK2*f1_*mvaD*f1, and pBBRM1MCS-2_*ispA*f1 from *E. kingsejongensis* Gf1	This study
MVA15	XL1-Blue harboring pUCM_*ERG9*SC from *S. cerevisiae* AH109, pSTVM_*mvaS*f1_*mvaE*f1_*mvaK1*f1_*mvaK2*f1_*mvaD*f1, and pBBRM1MCS-2_*idif*1_*ispA*f1 from *E. kingsejongensis* Gf1	This study
MVA16	XL1-Blue harboring pUCM_*crtE*PA_*crtB*PA_*crtI*PA_*crtY*PA from *P. agglomerans*	This study
MVA17	XL1-Blue harboring pUCM_*crtE*PA_*crtB*PA_*crtI*PA_*crtY*PA from *P. agglomerans* and pSTVM_*mvaS*f1_*mvaE*f1_*mvaK1*f1_*mvaK2*f1_*mvaD*f1 from *E. kingsejongensis* Gf1	This study
MVA18	XL1-Blue harboring pUCM_*crtE*PA_*crtB*PA_*crtI*PA_*crtY*PA from *P. agglomerans* and pBBRM1MCS-2_*idif*1 from *E. kingsejongensis* Gf1	This study
MVA19	XL1-Blue harboring pUCM_*crtE*PA_*crtB*PA_*crtI*PA_*crtY*PA from *P. agglomerans* and pBBRM1MCS-2_*idif*1_*ispA*f1 from *E. ingsejongensis* Gf1	This study
MVA20	XL1-Blue harboring pUCM_*crtE*PA_*crtB*PA_*crtI*PA_*crtY*PA from *P. agglomerans*, pSTVM_*mvaS*f1_*mvaE*f1_*mvaK1*f1_*mvaK2*f1_*mvaD*f1 and pBBRM1MCS-2_*idif*1 from *E. kingsejongensis* Gf1	This study
MVA21	XL1-Blue harboring pUCM_*crtE*PA_*crtB*PA_*crtI*PA_*crtY*PA from *P. agglomerans*, pSTVM_*mvaS*f1_*mvaE*f1_*mvaK1*f1_*mvaK2*f1_*mvaD*f1 and pBBRM1MCS-2_*idif*1_*ispA*f1 from *E. kingsejongensis* Gf1	This study
Plasmids		
pUCM	Cloning vector modified from pUC19; constitutive *lac* promoter, Ap	(Kim et al., 2010)
pUCM-mvaEf1	Constitutively expressed *mvaE* gene from *E. kingsejongensis* Gf1	This study
pUCM-mvaSf1	Constitutively expressed *mvaS* gene from *E. kingsejongensis* Gf1	This study
pUCM-mvaK1f1	Constitutively expressed *mvaK1* gene from *E. kingsejongensis* Gf1	This study
pUCM-mvaK2f1	Constitutively expressed *mvaK2* gene from *E. kingsejongensis* Gf1	This study
pUCM-mvaDf1	Constitutively expressed *mvaD* gene from *E. kingsejongensis* Gf1	This study
pUCM-ERG9SC	Constitutively expressed *ERG9* gene from *S. cerevisiae* AH109	This study
pUCM_idi$_{JM}$	Constitutively expressed *idi* gene from JM109	(Kong et al., 2015)
pUCM_ispA$_{T10}$	Constitutively expressed *ispA* gene from Top10	(Kong et al., 2015)
pUCM_idi$_{Gf1}$	Constitutively expressed *idi* gene from *E. kingsejongensis* Gf1	This study
pUCM_ispA$_{Gf1}$	Constitutively expressed *ispA* gene from *E. kingsejongensis* Gf1	This study
pUCM_crtMSA	Constitutively expressed *crtM* gene from *S. aureus*	(Kim et al., 2016)
pUCM_crtNSA	Constitutively expressed *crtN* gene from *S. aureus*	(Kim et al., 2016)

(*continued on next page*)

Table 1 (*continued*)

Strains and plasmids	Relevant properties	Source or reference
pUCM_crtEPA_crtBPA_crtIPA_crtYPA	Constitutively expressed *crtE*, *crtB*, *crtI*, and *crtY* genes from *P. agglomerans*	(Song et al., 2012)
pSTVM	Expression vector modified from pSTV28; deleted *lacZα* fragment and *lac* promoter, Cm	This study
pSTVM-mvaEf1	Constitutively expressed *mvaE* gene from *E. kingsejongensis* Gf1	This study
pSTVM-mvaSf1	Constitutively expressed *mvaS* gene from *E. kingsejongensis* Gf1	This study
pSTVM-mvaK1f1	Constitutively expressed *mvaK1* gene from *E. kingsejongensis* Gf1	This study
pSTVM-mvaK2f1	Constitutively expressed *mvaK2* gene from *E. kingsejongensis* Gf1	This study
pSTVM-mvaDf1	Constitutively expressed *mvaD* gene from *E. kingsejongensis* Gf1	This study
pSTVM-mvaEf1-mvaSf1	Constitutively expressed *mvaE* and *mvaS* genes from *E. kingsejongensis* Gf1.	This study
pSTVM-mvaK1f1-mvaK2f1	Constitutively expressed *mvaK1* and *mvaK2* genes from *E. kingsejongensis* Gf1	This study
pSTVM-mvaK1f1- mvaDf1	Constitutively expressed *mvaK1* and *mvaD* genes from *E. kingsejongensis* Gf1	This study
pSTVM-mvaK2f1-mvaDf1	Constitutively expressed *mvaK2* and *mvaD* genes from *E. kingsejongensis* Gf1	This study
pSTVM-mvaK1f1-mvaK2f1-mvaDf1	Constitutively expressed *mvaK1*, *mvaK2*, and *mvaD* genes from *E. kingsejongensis* Gf1	This study
pSTVM-mvaEf1-mvaSf1-mvaK1f1-mvaK2f1-mvaDf1	Constitutively expressed *mvaE*, *mvaS*, *mvaK1*, *mvaK2*, and *mvaD* genes from *E. kingsejongensis* Gf1	This study
pBBR1MCS-2	Cloning vector, comparable with pMB1 and p15A	(Kovach et al., 1995)
pBBR-crtMSA	Constitutively expressed *crtM* gene from *S. aureus*	This study
pBBR-crtNSA	Constitutively expressed *crtN* gene from *S. aureus*	This study
pBBR-crtMSA-crtNSA	Constitutively expressed *crtM* and *crtN* genes from *S. aureus*	This study
pBBR_idi$_{JM}$	Constitutively expressed *idi* gene from JM109	(Kong et al., 2015)
pBBR_ispA$_{T10}$	Constitutively expressed *ispA* gene from Top10	(Kong et al., 2015)
pBBR_idi$_{JM}$_ispA$_{T10}$	Constitutively expressed *idi* gene from JM109 and *ispA* gene from Top10	(Kong et al., 2015)
pBBR_idi$_{Gf1}$	Constitutively expressed *idi* gene from *E. kingsejongensis* Gf1	This study
pBBR_ispA$_{Gf1}$	Constitutively expressed *ispA* gene from *E. kingsejongensis* Gf1	This study
pBBR_idi$_{Gf1}$_ispA$_{Gf1}$	Constitutively expressed *idi* and *ispA* genes from *E. kingsejongensis* Gf1	This study

ispA$_{f1}$, and were assembled into the pBBR1MCS2 vector to construct pBBR1MCS2-idi$_{f1}$, pBBR1MCS2-ispA$_{f1}$, and pBBR1MCS2-idi$_{f1}$-ispA$_{f1}$ (Table 1). In addition, two MVA upstream pathway genes (mvaS$_{Ef}$ or mvaE$_{Ef}$) of *E. faecalis* KCTC3206 were engineered to be expressed in the pUCM vector, leading to development of pUCM-mvaS$_{Ef}$ and pUCM-mvaE$_{Ef}$, and assembled into the pSTVM vector, to construct pSTVM-mvaE$_{Ef}$, pSTVM-mvaS$_{Ef}$, and pSTVM-mvaE$_{Ef}$-mvaS$_{Ef}$. Moreover, pBBR1MCS2-idi$_{JM}$, pBBR1MCS2-ispA$_{T10}$, and pBBR1MCS2-idi$_{JM}$-ispA$_{T10}$ were used (Kong et al., 2015). *E. coli* was grown in Luria-Bertani (LB) medium at 37 °C for gene cloning, in TT medium at 30 °C for mevalonate production, and in Terrific broth (TB) medium at 30 °C for C$_{30}$, C$_{40}$ carotenoids, and squalene production on a rotary shaker at 250 rpm. Ampicillin (100 μg/mL), chloramphenicol (50 μg/mL), and kanamycin (30 μg/mL) (Sigma Aldrich, USA) were added to the culture as required.

2.2. Strain construction

The strains used in this study are listed in Table 1. To investigate the function of the engineered *E. kingsejongensis* Gf1 MVA upstream pathway in *E. coli*, recombinant *E. coli* MVA1 harboring pUCM-mvaE$_{f1}$ + pSTVM-mvaS$_{f1}$, *E. coli* MVA2 harboring pUCM-mvaS$_{f1}$ + pSTVM-mvaE$_{f1}$, *E. coli* MVA3 harboring pSTVM-mvaS$_{f1}$-mvaE$_{f1}$, and *E. coli* MVA4 harboring pUCM-mvaS$_{f1}$-mvaE$_{f1}$ were constructed, and MVA5, which overexpressed the upstream pathway genes of *E. faecalis* KCTC 3206 (pUCM-mvaE$_{Ef}$ + pSTVM-mvaS$_{Ef}$), was prepared to compare the activities of MVA upstream pathway enzymes of *E. kingsejongensis* Gf1. For carotenoid expression, C$_{30}$ 4,4′-diaponeurosporene pathway modules (pBBR1MCS2-crtM$_{SA}$-crtN$_{SA}$) and C$_{40}$ β-carotene pathway modules (pUCM-crtE$_{PA}$-crtB$_{PA}$-crtI$_{PA}$-crtY$_{PA}$), the functions of which have already been confirmed in our previous study, were used in this study (Song et al., 2012; Kim et al., 2016) (Table 1). Two strains (MVA6 and MVA7) were constructed by transforming both 4,4′-diaponeurosporene and MVA downstream pathway modules (MVA6) and both β-carotene and MVA downstream pathway modules (MVA7). To validate the function of the *E. kingsejongensis* Gf1 whole

MVA pathway modules, squalene and β-carotene pathways were used as reporter pathways. Strain MVA8 was constructed by transforming pUCM-ERG9$_{SC}$ for expressing a squalene synthesis pathway, and strain MVA9 was constructed by transforming both pUCM-ERG9$_{SC}$ and pSTVM-mvaS$_{f1}$-mvaE$_{f1}$-mvaK1$_{f1}$-mvaK2$_{f1}$-mvaD$_{f1}$. In a similar manner, strain MVA16 was constructed by transforming pUCM-crtE$_{PA}$-crtB$_{PA}$-crtI$_{PA}$-crtY$_{PA}$ for expressing a β-carotene pathway, and strain MVA17 was constructed by transforming both pUCM-crtE$_{PA}$-crtB$_{PA}$-crtI$_{PA}$-crtY$_{PA}$ and pSTVM-mvaS$_{f1}$-mvaE$_{f1}$-mvaK1$_{f1}$-mvaK2$_{f1}$-mvaD$_{f1}$. Strains MVA10, MVA11, and MVA12 were constructed to investigate the effects of upregulation of prenyl pyrophosphate pathway by transforming MVA9 with *idi*$_{JM}$, *ispA*$_{T10}$, and both *idi*$_{JM}$ and *ispA*$_{T10}$ modules of *E. coli*, respectively, and strains MVA13, MVA14, and MVA15 were constructed by transforming MVA9 with *idi*$_{f1}$, *ispA*$_{f1}$, and both *idi*$_{f1}$ and *ispA*$_{f1}$ modules of *E. kingsejongensis* Gf1, respectively. Moreover, strain MVA18, which coexpressed *idi*$_{f1}$ and β-carotene pathway, MVA19, which coexpressed *idi*$_{f1}$, *ispA*$_{f1}$, and β-carotene pathway, MVA20, which coexpressed *idi*$_{f1}$, whole MVA pathway, and β-carotene pathway, and MVA21, coexpressed *idi*$_{f1}$, *ispA*$_{f1}$, whole MVA pathway, and β-carotene pathway, were prepared.

2.3. Mevalonate fermentation

The mevalonate-producing recombinant *E. coli* MVA1, MVA2, MVA3, MVA4, and MVA5 strains were used. For flask culture, TT medium (Tabata and Hashimoto, 2004) containing 20 g/L glucose (separately sterilized), 16 g/L K$_2$HPO$_4$, 5 g/L peptone, 1 g/L citric acid (anhydrous), 25 mg/L MgSO$_4$·7H$_2$O (separately sterilized), 50 mg/L FeSO$_4$·7H$_2$O (separately sterilized), and 8 mg/L thiamine·HCl (separately sterilized) (pH 7.2) was used. An overnight culture grown on LB medium at 30 °C was inoculated in a flask containing 50 mL TT medium and cultivated aerobically at 30 °C for 24 h. Ampicillin (100 μg/mL) and chloramphenicol (50 μg/mL) was added, as required. For production in a jar fermenter, J medium (Tabata and Hashimoto, 2004) containing 10 g/L glucose (separately sterilized), 7 g/L KH$_2$PO$_4$, 1 g/L NH$_4$Cl, 1 g/L peptone, 1 g/L citric acid (anhydrous), 10 mg/L MnSO$_4$·7H$_2$O

(separately sterilized), 2 g/L MgSO₄·7H₂O (separately sterilized), 200 mg/L FeSO₄·7H₂O (separately sterilized), and 10 mg/L thiamine·HCl (separately sterilized) was used. Overnight culture in 100 mL TT medium in a 500-mL flask at 30 °C was transferred into a 2-L jar fermenter containing 1 L J medium and cultivated at 32 °C with agitation rate of 900 rpm and pO₂ concentration of 30%. During cultivation, pH was maintained at 7 using 14% (v/v) NH₄OH. Glucose concentration in medium was measured with HPLC-RID (Agilent, USA). For analysis of glucose concentration in culture broth, the collected culture broth filtrate was filtered using 0.2 μm syringe membrane filter, and 20 μL solution was injected for analysis with Agilent 1260 infinity high performance liquid chromatography (HPLC) instrument equipped with an Aminex HPX-87H column (300 × 7.8 mm; Bio-rad, USA) and a Agilent 1200 series refractive index detector (RID). Isocratic elution was done with DDW with 4 N H₂SO₄; flow rate was 1.0 mL/min. Retention time and concentration of glucose was quantified based on a calibration curve generated using various known concentrations of glucose (Bio basic, USA). The results represent the means from three independent determinations. When the initial glucose was depleted, glucose solution (500 g/L) was added continuously to keep the glucose concentration at approximate 10 g/L. Ampicillin (100 μg/mL) and chloramphenicol (50 μg/mL) was added before initiating the culture. Cell growth was monitored by measuring the optical density of culture broth at a wavelength of 600 nm (OD₆₀₀) using SPECTRAmax PLUS spectrophotometer (Bio-rad, USA).

2.4. Extraction and analysis of mevalonate and mevalonolactone

The concentration of mevalonate was determined by Agilent 7890A gas chromatography system equipped with an Agilent 5975 mass spectrometry detector (GC–MS) (Agilent, USA). The column used was DB SELECT 624UI from Agilent (0.25 mm i.d, 30 m length, 0.25 μm film thickness). Spectra were obtained under 70 eV EI condition. Helium was used at a flow rate of 1.0 mL/min. Injection was made by splitless mode. The oven temperature was initially held at 70 °C for 1 min, raised 3 °C/min to 190 °C, and 15 °C/min to 250 °C. Detector and injector temperatures were 250 °C. For analysis of mevalonate production in culture broth, the pH of the collected culture broth filtrate was maintained at 2 with 3 M HCl and incubated at 45 °C for 1 h to convert mevalonate to mevalonolactone, and saturated with anhydrous Na₂SO₄. After extraction of mevalonate with ethyl acetate, the solvent layer was analyzed for mevalonolactone levels. The concentration of mevalonolactone was quantified based on a calibration curve generated from various known concentrations of mevalonolactone (Sigma Aldrich, USA). The results represent means from three independent determinations.

2.5. Production, extraction, and analysis of 4,4′-diaponeurosporene, β-carotene, and squalene

The squalene producing recombinant *E. coli* MVA8, MVA9, MVA10, MVA11, MVA12, MVA13, MVA14, and MVA15 strains, 4,4′-diaponeurosporene producing recombinant *E. coli* MVA6 and MVA7, and β-carotene producing recombinant *E. coli* MVA16, MVA17, MVA18, MVA19, MVA20, and MVA21 strains were used. For flask culture, LB medium containing 5 g/L NaCl, 5 g/L yeast extract, and 10 g/L tryptone and TB medium containing 5 g/L glycerol, 12 g/L yeast extract, and 24 g/L tryptone were used. An overnight culture grown on LB medium at 30 °C was inoculated in a flask containing 50 mL TB medium and cultivated aerobically at 30 °C for 120 h. Ampicillin (100 μg/mL), chloramphenicol (50 μg/mL), and kanamycin (30 μg/mL) (Sigma Aldrich, USA) were added, as required. Thin layer chromatography (TLC) analysis was performed for initial analysis under 100% hexane solvent system which was similar to the condition described in our previous study (Lee et al., 2003). Carotenoid products were analyzed using a spectrophotometer with extracted product at room temperature

to monitor the change in absorbance at 468 nm for 4,4′-diaponeurosporene and 453 nm for β-carotene. Extracted carotenoids were prepared with acetone by two phase extraction. After centrifugation at 13000 rpm for 10 min, harvested pellets were resuspended in 1 mL acetone. Resuspended samples were extracted with sonication at 50 °C for 30 min. After centrifugation at 13000 rpm for 5 min, 500 μL supernatants were analyzed using a spectrophotometer at 468 nm and 453 nm. For more accurate quantification of the carotenoid products, HPLC-DAD (Agilent, USA) was used for detection and quantification of expressed carotenoids. The carotenoids were extracted with acetone by two phase extraction. After centrifugation at 4000 rpm for 30 min, harvested pellet was resuspended with 10 mL acetone. Resuspended pellet was disrupted with sonication at 50 °C for 30 min. Equal volume of hexane and DDW were added into the acetone extract, and upper solvent layer was transferred into the new glass tube. After drying with N₂ gas, the pellet was resuspended in 1 mL ethyl acetate and a 20 μL solution was injected for analysis with Agilent 1260 infinity high performance liquid chromatography (HPLC) instrument equipped with a Zorbex Eclips XDB-C18 column (4.6 × 150 mm, 5.0 μm; Agilent, USA) and an Agilent 1200 series diode-array detector (DAD). The HPLC conditions used were as follows: λ-max 210 nm for squalene, 453 nm for β-carotene; isocratic elution with acetonitrile-methanol-isopropanol (8:1.5:0.5, v/v); flow rate of 1.0 mL/min. Retention time and concentrations of extracted squalene and β-carotene were confirmed using squalene and β-carotene (Sigma Aldrich, USA). The results represent the means from three independent determinations.

3. Results and discussion

3.1. Function of the E. kingsejongensis Gf1 MVA upstream pathway module

To analyze the function of the engineered *E. kingsejongensis* Gf1 MVA upstream pathway in *E. coli*, recombinant *E. coli* MVA1, MVA2, MVA3, and MVA4 were used. As the MVA upstream pathway can synthesize MVA if functionally expressed in *E. coli* (Fig. 1), identification and quantification of MVA were performed in all four strains cultured with 50 mL LB medium in 250-mL flasks at 30 °C for 24 h. For all four strains expressing the *E. kingsejongensis* Gf1 MVA upstream pathway, MVA was identified in the culture media (Fig. 2a), indicating functional expression of both *mvaE* and *mvaS* of *E. kingsejongensis* Gf1 in *E. coli*. Among the four strains tested, the strain MVA1 produced the highest amount of MVA (~ 4.1 g/L) compared to the other three strains (Fig. 2b). The difference in levels of MVA between MVA1 and the others could be explained by the higher expression of *mvaE* on the high copy number vector, pUCM, than that of *mvaS* on the low copy number vector, pSTVM. The previous studies revealed that accumulation of HMG-CoA causes inhibition in cell growth (Pitera et al., 2007) and heterologous protein expression level was affected by plasmid copy number (Schendel et al., 1989; Segall-Shapiro et al., 2018). In comparison to the wild type *E. coli* XL1-Blue, strain MVA1 had no effect on cell growth. However, cell growth of strains MVA3 and MVA4 slightly decreased and strain MVA2 showed severe growth inhibition. These results suggested that fine tuning of expressions of *mvaS* and *mvaE* genes for detoxifying HMG-CoA accumulation is one of the important factors in MVA production. (Ma et al., 2011). Based on these results, the functional activity of MVA upstream enzymes from *E. kingsejongensis* Gf1 was verified by comparing with the enzymes from *E. faecalis* KCTC 3206. The complementation of modulated enzymes from *E. kingsejongensis* Gf1 and *E. faeclais* KCTC 3296, including pUCM-mvaE₍f1₎ + pSTVM-mvaS₍f1₎, pUCM-mvaE₍f1₎ + pSTVM-mvaS₍Ef₎, pUCM-mvaE₍Ef₎ + pSTVM-mvaS₍f1₎, and pUCM-mvaE₍Ef₎ + pSTVM-mvaS₍Ef₎, revealed that activities of MVA upstream pathway enzymes from *E. kingsejongensis* Gf1 were higher than that of *E. faeclais* KCTC 3296 via mevalonate production (4.3, 3.8, 3.1, and 2.9 mg/L, respectively).

Next, to investigate the effect of glucose concentration on MVA formation kinetics, bioreactor batch fermentation of strain MVA1 was
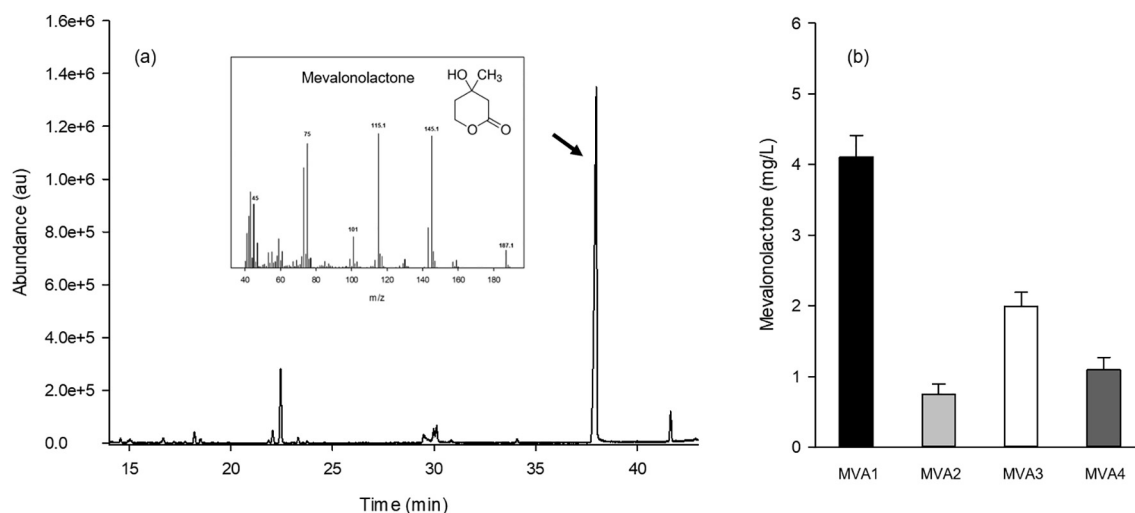
Fig. 2. Analysis of function of the *E. kingsejongensis* Gf1 MVA upstream pathway modules. (a) Gas chromatography-mass spectrometry (GC–MS) analysis of mevalonolactone converted from mevalonate in *E. coli* strains. (b) Production of mevalonolactone converted from mevalonate in recombinant *E. coli* strains MVA1, MVA2, MVA3, and MVA4.

performed with three different glucose concentrations (20, 30, and 40 g/L). Increase in cell growth and MVA production was proportional to increasing glucose concentration: strain MVA1 could grow up to 27.2, 44.4, and 48.5 of OD_{600}, and MVA levels increased to 11.2, 14.7, and 17.3 g/L at glucose concentration of 20, 30, and 40 g/L, respectively. However, the MVA yields (g-MVA/g-glucose) gradually decreased with increasing glucose concentrations (0.56, 0.49, and 0.43 g-MVA/g-glucose at 20, 30, and 40 g/L glucose, respectively). These inverse results between the production and yields were generally observed because of the unoptimized culture condition and production of byproducts (Yang et al., 2013; Fonseca et al., 2019). Hence, high glucose concentration promoted high levels of organic acids, such as acetic acid or lactic acid. In turn, low glucose concentration reduced organic acids production and promoted MVA production. Thus, proper concentration of substrates leads to optimal MVA production.

To investigate whether MVA production could further increase by adding glucose, fed-batch fermentation of strain MVA1 was conducted together with a control strain MVA5. Although maximum cell growth was comparable (39.9 of OD_{600} of strain MVA1 vs. 36.4 of OD_{600} of strain MVA5), MVA1 strain produced more MVA than MVA5 strain (52.5 vs. 34.7 g/L; Fig. 3). Both productivity (0.81 g/L/h) and MVA conversion yield (0.31 g/g of glucose) of the *E. kingsejongensis* Gf1 MVA upstream pathway was higher than those of *E. faecalis* KCTC 3206 MVA upstream pathway (0.54 g/L/h and 0.22 g/g of glucose, respectively). These results also indicated that the activity of the *E. kingsejongensis* Gf1 MVA upstream pathway enzymes is higher than that of *E. faecalis* KCTC

3206 MVA upstream pathway enzymes. By controlling feeding rate to maintain the glucose concentration under 10 g/L, acetic acid formation was not observed until after 65 h of culture.

3.2. Function of the E. kingsejongensis Gf1 MVA downstream pathway module

To determine whether the MVA downstream pathway modules of *E. kingsejongensis* Gf1 functioned properly, C_{30} 4,4′-diaponeurosporene and C_{40} β-carotene pathway modules, as reporters, were linked to the MVA downstream pathway modules (Song et al., 2012; Kim et al., 2016) (Fig. 1). Strains MVA6 and MVA7 were grown in TB medium supplemented with exogenous MVA. MVA6 strain grown in media supplemented with different MVA concentrations (0, 10, 20, and 40 mM) increased 4,4′-diaponeurosporene production in parallel with increasing MVA concentration except for 40 mM MVA. However, cell growth was inhibited by increasing exogenous MVA concentration. The observed cell growth inhibition could be explained by toxic effect of accumulating intermediates including IPP, FPP, or GGPP (Martin et al., 2003; George et al., 2018). However, these results indicated that exogenous MVA was successfully used as a substrate of the *E. kingsejongensis* Gf1 MVA downstream pathway enzymes, indicating the functional expression of the MVA downstream pathway enzymes in *E. coli*. As supplementation with 20 mM MVA produced highest amount of 4,4′-diaponeurosporene in MVA6 strain, the MVA7 strain was subjected to 20 mM MVA to confirm the effect of the *E. kingsejongensis* Gf1 MVA
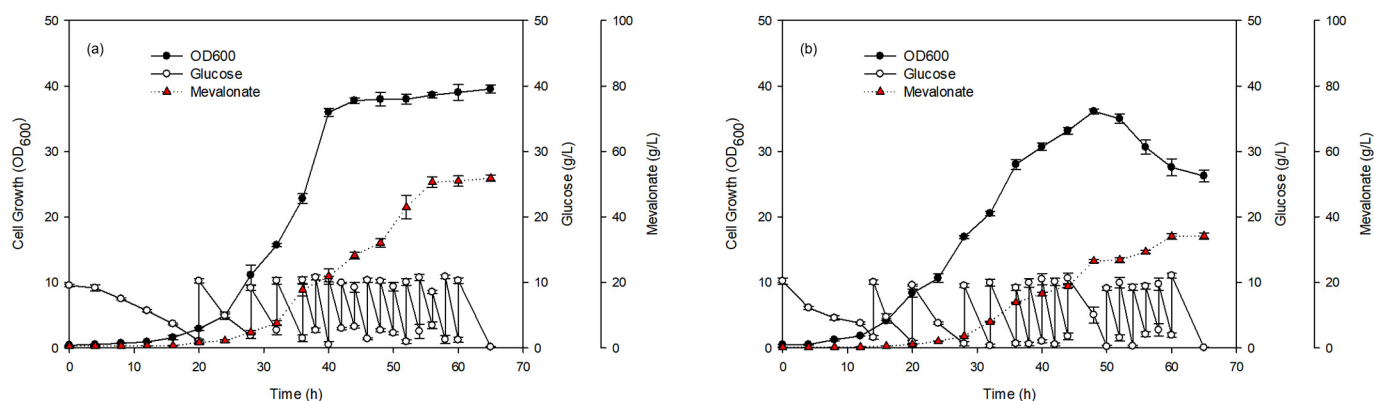

Fig. 3. Fed-batch fermentation of strains MVA1 (a) and MVA5 (b). Glucose feeding rate was regulated to maintain the glucose concentration under 10 g/L.
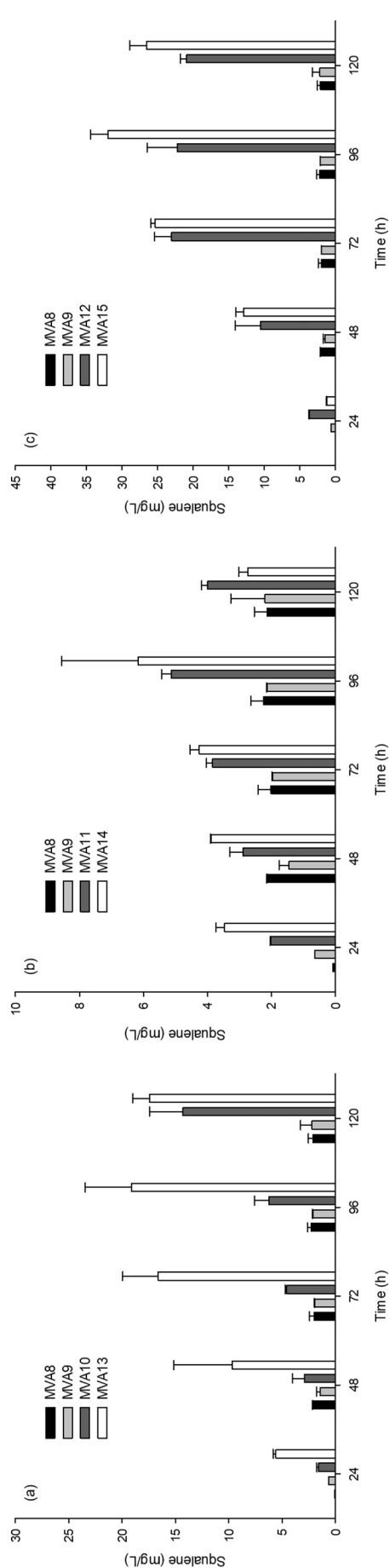
Fig. 4. Squalene production by strains MVA8, MVA9, MVA10, MVA11, MVA12, MVA13, MVA14, and MVA15. (a) Effect of overexpression of *ispA* from *E. coli* and *E. kingsejongensis* Gf1 on squalene production, (b) Effect of overexpression of *idi* from *E. coli* and *E. kingsejongensis* Gf1 on squalene production, (c) Effect of overexpression of both *idi* and *ispA* from *E. coli* and *E. kingsejongensis* Gf1 on squalene production.

downstream pathway enzymes on carotenoid production. Compared with control, the supplementation of 20 mM MVA enhanced 4,4′-diaponeurosporene production by 1.4-fold and β-carotene production by 1.6-fold.

3.3. Isoprenoid production in E. coli expressing the E. kingsejongensis Gf1 whole MVA pathway module

Strains MVA8, MVA9, MVA16, and MVA17 were used to verify the function of the *E. kingsejongensis* Gf1 whole MVA pathway modules with squalene and β-carotene production as an indicator. In flask cultures, although whole mevalonate pathway modules were introduced, squalene production of MVA9 (2.2 mg/L) was similar to that of MVA8 (2.14 mg/L) after 120 h of culture (Fig. 4), and β-carotene production of MVA17 (1.82 mg/L) was lower than that of MVA16 (5.16 mg/L) after 120 h of culture (Fig. 5). Similar to the observed effect of 40 mM MVA supplementation, this unexpected result might be due to unbalanced metabolic flux in the engineered pathways causing accumulation of intermediates, such as HMG-CoA, mevalonate, and prenyl pyrophosphates (Pitera et al., 2007; George et al., 2018) (Fig. 1). Mevalonate kinase 1 (mvaK1) has been reported as one of the key enzymes in MVA pathway, and regulated by prenyl pyrophosphate metabolism (Tricarico et al., 2015). To investigate the effects of upregulation of prenyl pyrophosphate pathway, strains MVA10, MVA11, and MVA12 were used. As expected, cell growth, squalene, and β-carotene productions were enhanced in all strains (Figs. 4 and 5), especially expression of *idi* modules, which has been reported as the key enzyme for terpenoid production in *E. coli* showed the highest effect (Ghimire et al., 2009; Zhao et al., 2013; Lv et al., 2013). MVA10, MVA11, and MVA12 strains produced 14.3, 2.13, and 22.2 mg/L squalene, respectively, while MVA 13, MVA14, and MVA15 strains produced 19.1, 6.16, and 32.0 mg/L squalene after 120 h of culture, respectively (Fig. 4). This result suggested that upregulation of prenyl pyrophosphate pathway would alleviate growth inhibition and enhance squalene production by balancing whole mevalonate and prenyl pyrophosphate pathway flux (Zhou et al., 2015). Similar positive effect was also observed on β-carotene production (Fig. 5). MVA18 and MVA19 strains produced 10.55 and 11.43 mg/L β-carotene after 120 h of cultures, respectively (Fig. 5). Furthermore, enhanced β-carotene productions of 12.1 mg/L and 12.6 mg/L were observed in both MVA20 and MVA21 strains (Fig. 5). Altogether, it is clear that the expression of heterologous *E. kingsejongensis* Gf1 MVA pathway modules enhances isoprenoid production (squalene and carotenoids) in *E. coli*. These results suggested that MVA and prenyl pyrophosphate pathway genes of *E. kingsejongensis* Gf1 are excellent candidates that can be employed for production of the value-added biochemicals. However, the yields of products here can be further elevated through additional engineering. To achieve optimal application of heterologous *E. kingsejongensis* Gf1 MVA pathway, effective redox and energy balancing, fine tuning of pathway enzymes, and metabolic flux optimization are required.

4. Conclusions

In summary, the new MVA and IPP pathway enzymes of *E. kingsejongensis* Gf1 were functionally expressed in the heterologous host *E. coli* and their activities were higher than those of *E. faecalis* KCTC 3206 and *E. coli*. Moreover, the results demonstrated that balancing metabolic flux is one of the important factors in optimization of isoprenoid production in microbial hosts engineered for the heterologous pathways. This study provides a model system for engineering microbial hosts for production of bioactive materials from bioresources, such as crude glycerol wastes.

Declaration of Competing Interest

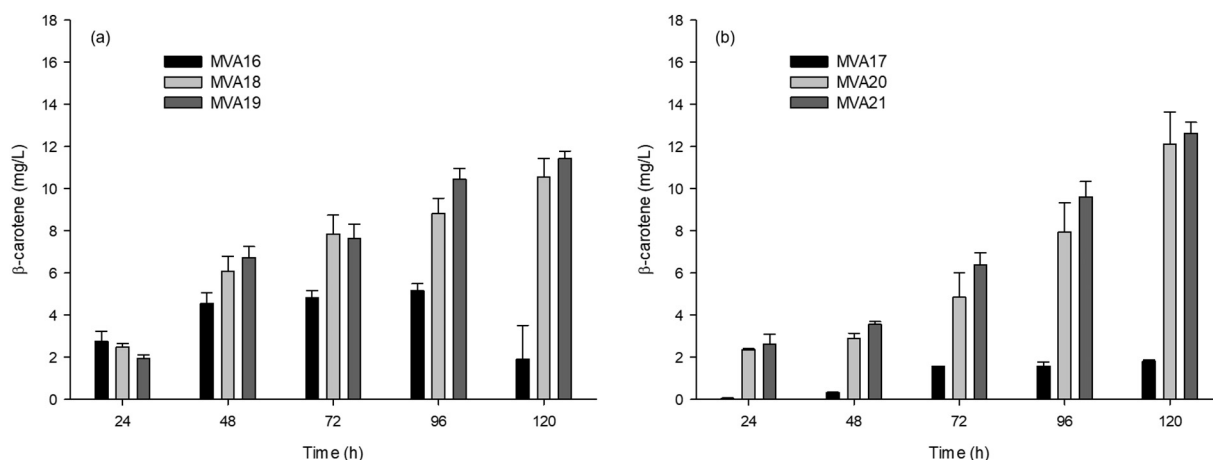The authors declare that they have no conflict of interest.

Fig. 5. β-carotene production by strains MVA16, MVA17, MVA18, MVA19, MVA20, and MVA21. (a) Effect of overexpression of *idi or/and ispA* from *E. kingsejongensis* Gf1 on β-carotene production of strains MVA16, MVA18, and MVA19 (without whole MVA pathway expression) (b) Effect of overexpression of *idi or/and ispA* from *E. kingsejongensis* Gf1 on β-carotene production of strains MVA17, MVA20, and MVA21 (with whole MVA pathway expression).

Acknowledgements

Appendix A. Supplementary data

Supplementary figures for 1) the growth of strains expressing MVA pathway enzymes, 2) effect of initial glucose concentration on the growth of strain MVA1, 3) function of MVA downstream pathway of *E. kingsejongensis* Gf1, 4) production of carotenoids supplemented with or without exogenous MVA, and 5) the growth of strains expressing an IPP pathway enzyme are available in online version of the paper. Supplementary data to this article can be found online at https://doi.org/10.1016/j.biteb.2019.100291.

References

Chaudhary, N., Ngadi, M.O., Simpson, B., 2012. Comparison of glucose, glycerol and crude glycerol fermentation by *Escherichia coli* K12. J. Bioproces. Biotechniq. S1. https://doi.org/10.4172/2155-9821.S1-001.

Connolly, D.M., Winkler, M.E., 1989. Genetic and physiological relationships among the miaA gene, 2-methylthio-N6-(delta 2-isopentenyl)-adenosine tRNA modification, and spontaneous mutagenesis in *Escherichia coli* K-12. J. Biotechnol. 171 (6), 3233–3246.

Fonseca, B.C., Schmidell, W., Reginatto, V., 2019. Impact of glucose concentration on productivity and yield of hydrogen production by the new isolate *Clostridium beijerinckii* Br21. Can. J. Chem. Eng. 97 (5), 1092–1099.

George, K.W., Thompson, M.G., Kim, J., Baidoo, E.E.K., Wang, G., Benites, V.T., Petzold, C.J., Chan, L.J.G., Yilmaz, S., Turhanen, P., Adams, P.D., Keasling, J.D., Lee, T.S., 2018. Integrated analysis of isopentenyl pyrophosphate (IPP) toxicity in isoprenoid-producing *Escherichia coli*. Metab. Eng. 47, 60–72.

Ghimire, G.P., Lee, H.C., Sohng, J.K., 2009. Improved squalene production via modulation of the methylerythritol 4-phosphate pathway and heterologous expression of genes from *Streptomyces peucetius* ATCC 27952 in *Escherichia coli*. Appl. Environ. Microbiol. 75 (22), 7291–7293.

Gliszczyńska, A., Niezgoda, N., Gładkowski, W., Świtalska, M., Wietrzyk, J., 2017. Isopropanol-phospholipid conjugates as potential therapeutic agents: synthesis, characterization and antiproliferative studies. PLoS One 12 (2), e0172238.

Hedl, M., Sutherlin, A., Wilding, E.I., Mazzulla, M., McDevitt, D., Lane, P., Burgner, J.W., Lehnbeuter, K.R., Stauffacher, C.V., Gwynn, M.N., Rodwell, V.W., 2002. *Enterococcus faecalis* acetoacetyl-coenzyme A thiolase/3-hydroxy-3-methylglutaryl-coenzyme A reductase, a dual-function protein of isopentenyl diphosphate biosynthesis. J. Bacteriol. 184 (8), 2116–2122.

Hung, K., Hu, X., Maimone, T.J., 2018. Total synthesis of complex terpenoids employing radical cascade processes. Nat. Prod. Rep. 35 (2), 174–202.

Hunter, W.N., 2007. The non-mevalonate pathway of isoprenoid precursor biosynthesis. J. Biol. Chem. 282 (30), 21573–21577.

Kim, S.H., Lee, P.C., 2012. Functional expression and extension of *staphylococcal* staphyloxanthin biosynthetic pathway in *Escherichia coli*. J. Biol. Chem. 287 (26), 21575–21583.

Kim, S.H., Park, Y.H., Schmidt-Dannert, C., Lee, P.C., 2010. Redesign, reconstruction, and directed extension of the *Brevibacterium linens* C40 carotenoid pathway in *Escherichia coli*. Appl. Environ. Microbiol. 76 (15), 5199–5206.

Kim, S.H., Kim, M.S., Lee, B.Y., Lee, P.C., 2016. Generation of structurally novel short carotenoids and study of their biological activity. Sci. Rep. 6, 21987.

Kong, M.K., Kang, H.J., Kim, J.H., Oh, S.H., Lee, P.C., 2015. Metabolic engineering of the Stevia rebaudiana ent-kaurene biosynthetic pathway in recombinant *Escherichia coli*. J. Biotechnol. 214, 95–102.

Kovach, M.E., Elzer, P.H., Hill, D.S., Robertson, G.T., Farris, M.A., Roop II, R.M., Peterson, K.M., 1995. Four new derivatives of the broad-host-range cloning vector pBBR1MCS, carrying different antibiotic-resistance cassettes. Geen 166 (1), 175–176.

Lee, P.C., Schmidt-Dannert, C., 2002. Metabolic engineering towards biotechnological production of carotenoids in microorganisms. Appl. Microbiol. Biotechnol. 60 (1–2), 1–11.

Lee, P.C., Momen, A.Z.R., Mijts, B.N., Schmidt-Dannert, C., 2003. Biosynthesis of structurally novel carotenoids in *Escherichia coli*. Chem. Biol. 10 (5), 453–462.

Lee, P.C., Salomon, C., Mijts, B., Schmidt-Dannert, C., 2008. Biosynthesis of ubiquinone compounds with conjugated prenyl side chains. Appl. Environ. Microbiol. 74 (22), 6908–6917.

Li, M., Nian, R., Xian, M., Zhang, H., 2018. Metabolic engineering for the production of isoprene and isopentenol by *Escherichia coli*. Appl. Microbiol. Biotechnol. 102 (18), 7725–7738.

Li, L., Wang, X., Li, X., Shi, H., Wang, F., Zhang, Y., Li, X., 2019. Combinatorial engineering of mevalonate pathway and diterpenoid synthases in *Escherichia coli* for cis-abienol production. J. Agric. Food Chem. 67 (23), 6523–6531.

Liu, C.L., Bi, H.R., Fan, L.H., Tan, T.W., 2019. Engineering and manipulation of a mevalonate pathway in *Escherichia coli* for isoprene production. Appl. Microbiol. Biotechnol. 103 (1), 239–250.

Lv, X., Xu, H., Yu, H., 2013. Significantly enhanced production of isoprene by ordered coexpression of genes dxs, dxr, and idi in *Escherichia coli*. Appl. Microbiol. Biotechnol. 97 (6), 2357–2365.

Ma, S.M., Garcia, D.E., Redding-Johanson, A.M., Friedland, G.D., Chan, R., Batth, T.S., Haliburton, J.R., Chivian, D., Keasling, J.D., Petzold, C.J., Lee, T.S., Chhabra, S.R., 2011. Optimization of a heterologous mevalonate pathway through the use of variant HMG-CoA reductases. Metab. Eng. 13 (5), 588–597.

Martin, V.J., Pitera, D.J., Withers, S.T., Newman, J.D., Keasling, J.D., 2003. Engineering a mevalonate pathway in *Escherichia coli* for production of terpenoids. Nat. Biotechnol. 21 (7), 796–802.

Miziorko, H.M., 2011. Enzymes of the mevalonate pathway of isoprenoid biosynthesis. Arch. Biochem. Biophys. 505 (2), 131–143.

Pitera, D.S., Paddon, C.J., Newman, J.D., Keasling, J.D., 2007. Balancing a heterologous mevalonate pathway for improved isoprenoid production in *Escherichia coli*. Metab. Eng. 9 (2), 193–207.

Sadhukhan, S., Villa, R., Sarkar, U., 2016. Microbial production of succinic acid using crude and purified glycerol from a *Crotalaria juncea* based biorefinery. Biotechnol. Rep. 10, 84–93.

Schendel, F.J., Baude, E.J., Flickinger, M.C., 1989. Determination of protein expression and plasmid copy number from cloned genes in *Escherichia coli* by flow injection analysis using an enzyme indicator vector. Biotechnol. Bioeng. 34 (8), 1023–1036.

Segall-Shapiro, T.H., Sontag, E.D., Voigt, C.A., 2018. Engineered promoters enable constant gene expression at any copy number in bacteria. Nat. Biotechnol. 36, 352–358.

Song, G.H., Kim, S.H., Choi, B.H., Han, S.J., Lee, P.C., 2012. Heterologous carotenoid-biosynthetic enzymes functional complementation and effects on carotenoid profiles in *Escherichia coli*. Appl. Environ. Microbiol. 79 (2), 610–618.

Tabata, K., Hashimoto, S.I., 2004. Production of mevalonate by a metabolically-engineered *Escherichia coli*. Biotechnol. Lett. 26 (19), 1487–1491.

Tholl, D., 2015. Biosynthesis and biological functions of terpenoids in plants. Adv. Biochem. Eng. Biotechnol. 146, 63–106.

Tricarico, P.M., Crovella, S., Celsi, F., 2015. Mevalonate pathway blockade,

mitochondrial dysfunction and autophagy: a possible link. Int. J. Mol. Sci. 16 (7), 16067–16084.

Wang, C., Zada, B., Wei, G., Kim, S.W., 2017. Metabolic engineering and synthetic biology approaches driving isoprenoid production in *Escherichia coli*. Bioresour. Technol. 241, 430–438.

Ward, V.C.A., Chatzivasileiou, A.O., Stephanopoulos, G., 2018. Metabolic engineering of *Escherichia coli* for the production of isoprenoids. FEMS Microbiol. Lett. 365 (10). https://doi.org/10.1093/femsle/fny079.

Yang, J., Xian, M., Su, S., Zhao, G., Nie, Q., Jiang, X., Zheng, Y., Liu, W., 2012. Enhancing production of bio-isoprene using hybrid MVA pathway and isoprene synthase in *E. coli*. PLoS One 7 (4), e33509.

Yang, X., Tu, M., Xie, R., Adhikari, S., Tong, Z., 2013. A comparison of three pH control methods for revealing effects of undissociated butyric acid on specific butanol production rate in batch fermentation of *Clostridium acetobutylicum*. AMB Express 3 (1). https://doi.org/10.1186/2191-0855-3-3.

Yang, S., Cao, Y., Sun, L., Li, C., Lin, X., Cai, Z., Zhang, G., Song, H., 2018. Modular pathway engineering of *Bacillus subtilis* to promote de novo biosynthesis of menaquinone-7. ACS Synth. Biol. 8 (1), 70–81.

Zhao, J., Li, Q., Sun, T., Zhu, X., Xu, H., Tang, J., Zhang, X., Ma, Y., 2013. Engineering central metabolic modules of *Escherichia coli* for improving beta-carotene production. Metab. Eng. 17, 42–50.

Zhou, J., Wang, C., Yang, L., Choi, E.S., Kim, S.W., 2015. Geranyl diphosphate synthase: an important regulation point in balancing a recombinant monoterpene pathway in *Escherichia coli*. Enzym. Microb. Technol. 68, 50–55.